Redox Biology 28 (2020) 101324

Contents lists available at ScienceDirect

Redox Biology

journal homepage: www.elsevier.com/locate/redox

Research Paper

Blockade of the trans-sulfuration pathway in acute pancreatitis due to nitration of cystathionine β-synthase

Sergio Rius-Pérez[a,1], Salvador Pérez[a,1], Isabel Torres-Cuevas[b], Pablo Martí-Andrés[a], Raquel Taléns-Visconti[c], Alberto Paradela[e], Laura Guerrero[e], Luis Franco[d,f], Gerardo López-Rodas[d,f], Luis Torres[d,f], Fernando Corrales[e], Juan Sastre[a,*]

[a] Department of Physiology, Faculty of Pharmacy, University of Valencia, 46100, Burjassot, Valencia, Spain
[b] Neonatal Research Group, Health Research Institute La Fe, Valencia, Spain
[c] Department of Pharmacy and Pharmaceutical Technology and Parasitology, University of Valencia, 46100, Burjassot, Valencia, Spain
[d] Department of Biochemistry and Molecular Biology, University of Valencia, 46100, Burjassot, Valencia, Spain
[e] Proteomics Unit, Centro Nacional de Biotecnología, CSIC, 28049, Madrid, Spain
[f] Institute of Health Research, INCLIVA, Valencia, Spain

ARTICLE INFO

Keywords:
Acute inflammation
S-adenosylmethionine
Homocysteine
Cystathionine β-synthase
Nitrosative stress

ABSTRACT

Acute pancreatitis is an inflammatory process of the pancreatic gland that may lead to dysregulation of the trans-sulfuration pathway. The aims of this work were firstly to study the methionine cycle as well as the trans-sulfuration pathway using metabolomic and proteomic approaches identifying the causes of this dysregulation in an experimental model of acute pancreatitis; and secondly to reveal the effects of S-adenosylmethionine administration on these pathways. Acute pancreatitis was induced by cerulein in mice, and a group of animals received S-adenosylmethionine treatment. Cerulein-induced acute pancreatitis rapidly caused marked depletion of methionine, S-adenosylmethionine, 5′-methylthioadenosine, cystathionine, cysteine, and glutathione levels in pancreas, but S-adenosylhomocysteine and homocysteine remained unchanged. Protein steady-state levels of S-adenosylhomocysteine-hydrolase and cystathionine gamma-lyase diminished but methylthioadenosine phosphorylase levels increased in pancreas with acute pancreatitis. Although cystathionine β-synthase protein levels did not change with acute pancreatitis, *Nos2* mRNA and protein levels were markedly up-regulated and caused tyrosine nitration of cystathionine β-synthase in pancreas. S-adenosylmethionine administration enhanced *Nos2* mRNA expression and cystathionine β-synthase nitration and triggered homocysteine accumulation in acute pancreatitis. Furthermore, S-adenosylmethionine administration promoted enrichment of the euchromatin marker H3K4me3 in the promoters of *Tnf-α, Il-6, and Nos2* and enhanced the mRNA up-regulation of these genes. Accordingly, S-adenosylmethionine administration increased inflammatory infiltrate and edema in pancreas with acute pancreatitis. In conclusion, tyrosine-nitration of cystathionine β-synthase blockades the trans-sulfuration pathway in acute pancreatitis promoting homocysteine accumulation upon S-adenosylmethionine treatment.

1. Introduction

Methionine is an essential sulfur amino acid that is not only involved in protein biosynthesis, but it also acts as a metabolic precursor for critical metabolic pathways [1,2]. It is the first precursor for synthesis of S-adenosylmethionine (SAM), the principal biological methyl donor in cells. Through this metabolic pathway, SAM donates its methyl group to a large variety of acceptors molecules including nucleic acids, proteins, and lipids. S-adenosylhomocysteine (SAH), the product of all trans-methylation reactions, is converted into homocysteine and next, homocysteine is remethylated into methionine to allow methionine recycling in cells [3,4]. Alternatively, SAM can be converted into decarboxylated SAM (dcSAM) to provide an aminopropyl group for the synthesis of polyamines [5]. On the other hand, using homocysteine as intermediary and through the trans-sulfuration pathway, methionine can also act as the primary source of cysteine, a limiting factor for the

* Corresponding author. Department of Physiology, School of Pharmacy, University of Valencia, Avda. Vicente Andres Estelles s/n, 46100, Burjasot, Valencia, Spain.
E-mail address: juan.sastre@uv.es (J. Sastre).
[1] Sergio Rius-Pérez and Salvador Pérez have contributed equally as first authors.

https://doi.org/10.1016/j.redox.2019.101324
Received 15 July 2019; Received in revised form 3 September 2019; Accepted 7 September 2019
Available online 08 September 2019

synthesis of reduced glutathione (GSH) [1]. Hence, methionine metabolism through the trans-sulfuration pathway and the trans-methylation system decisively contributes to the maintenance of redox homeostasis in cells [6]. Increased levels of homocysteine, a sign of dysregulation of the trans-sulfuration pathway, have been detected in plasma of patients with a variety of gastrointestinal disorders including inflammatory bowel disease [7,8], colorectal cancer [9] as well as acute pancreatitis [10].

Acute pancreatitis (AP) is an inflammatory process of the pancreatic gland that may eventually lead to systemic complications [11]. Pancreatic GSH depletion is an early feature in the development of acute pancreatitis, and this depletion when maintained in a long term contributes to the severity of the disease [12–14]. GSH depletion is not accompanied by increased levels of oxidized glutathione (GSSG) in experimental models of acute pancreatitis, but it is associated with protein cysteinylation and γ-glutamylcysteinylation, which was considered a subtype of oxidative stress called disulfide stress [15]. Furthermore, SAM levels decreased in pancreas during acute pancreatitis in rats [16]. Nevertheless, the precise mechanism involved in the dysregulation of the trans-sulfuration pathway in acute pancreatitis remains to be explored. In this work, firstly we have studied the methionine cycle as well as the trans-sulfuration pathway using metabolomic and proteomic approaches in an experimental model of acute pancreatitis identifying the causes of the dysregulation; secondly, we have detected the effects of SAM administration on these pathways.

2. Material and methods

2.1. Animals and experimental model of acute pancreatitis

Male C57BL/6J mice (Jackson Laboratory, Barcelona, Spain) were housed under standard environmental conditions, with food and water *ad libitum*. Experiments were conducted in compliance with the legislation on protection of animals used for scientific purposes in Spain (RD 53/2013) and the EU (Directive 2010/63/EU). Protocols were approved by the Ethics Committee of Animal Experimentation and Welfare of the University of Valencia (Valencia, Spain).

Acute pancreatitis was induced in 10-week-old mice. Mice received intraperitoneal injections of cerulein (Sigma-Aldrich, St. Louis, MO, USA) (50 μg/kg body weight) at 1 h intervals [17]. In the time-course study, animals were sacrificed 1 h after the first, third, fifth and seventh injections of cerulein. SAM (Sigma-Aldrich, St. Louis, MO, USA) was administered intraperitoneally (15 mg/kg body weight) 10 min before the first and fourth cerulein injections in one group of animals. Mice were euthanized under anesthesia with isoflurane 3–5%, subsequently were exsanguinated, and pancreas was immediately removed and used as described below. The sacrifice was confirmed by cervical dislocation.

2.2. Determination of trans-sulfuration pathway metabolites by UPLC-MS/MS

In the analysis of GSH, homocysteine, cysteine, cystathionine, methionine and serine levels, pancreatic tissues were homogenized in phosphate buffered saline (PBS) and 10 mmol/L N-ethylmaleimide (NEM) (Sigma-Aldrich, St. Louis, MO, USA) (pH 7.0), with a ratio of tissue and buffer of 1:4. On the other hand, to determine SAM, SAH and MTA levels, pancreatic samples were homogenized in 0.1% v/v HCOOH, adding 1 ml per 100 mg of tissue. Thereafter, perchloric acid solution was added to obtain a final concentration of 4% and samples were centrifuged at 11.000 rpm for 15 min at 4 °C. Finally, 95 μL of supernatants and 5 μL of internal standard (IS) solution (10 mmol L-1) were added and injected in the chromatographic system (UPLC-MS/MS).

The chromatographic system used consisted of a Waters Acquity UPLC-XevoTQ system (Milford, MA, USA). The conditions employed were: positive electrospray ionization (ESI), capillary voltage 3.50 kV, cone 20.00 V, extractor 5.00 V, source temperature 120 °C, desolvation temperature 300 °C, nitrogen cone and desolvation gas flows were 25 and 690 L h^{-1}, respectively. Separation conditions were selected to achieve appropriate chromatographic retention and resolution by using a kinetex UPLC C8 column (100 × 2.1 mm × 100 Å, 1.7 μm) from Phenomenex.

Table 1
Transitions for analytes determined by LC–MS/MS.

Analyte	*m/z* parent ion	Cone (v)	*m/z* daughter ion Quantification	Confirmation	Collision energy (eV)
GSH	433.2	30	304.3	201.2	15
Homocysteine	269.1	35	136.1	90	11
Cysteine	247.1	25	158.1	184.2	20
Cystathionine	223.2	20	88.1	134.1	15
Methionine	150.2	20	104.2	133.2	15
SAM	400.1	15	250.5	298.9	15
SAH	385.1	15	136.1	250.1	15
MTA	299.0	25	136.1	162.9	25
Serine	160.0	20	60.0	88.0	10

A binary gradient was used in which mobile phase A was 0.1% (v/v) HCOOH; Mobile phase B was acetonitrile (CH_3CN). The flow was 350 μL/min, the column temperature was 30 °C and the injection volume was 5 μL. The gradient started with 0% phase A, from 2.5 to 4.4 min, and the % of phase A increased to 65%. These conditions were maintained for 1.6 min to return to the initial conditions for 3.9 min, and then the system was rebalanced.

Mass spectrometric detection was carried out by multiple reaction monitoring (MRM) employing the acquisition parameters summarized in Table 1. Two MRM transitions per analyte were acquired for quantification and confirmation [18].

2.3. Protein quantification by MRM (see supplementary methods)

Mechanical disruption of pancreatic tissue was performed using a Potter-Elvehjem homogenizer, in the presence of 7 M urea, 2 M thiourea, 4% CHAPS, 40 mM DTT and protease inhibitor cocktail (Roche Diagnostics). Individual sample homogenates were centrifuged for 5 min at 10000 g and cleared supernatans stored at −80 °C until further processing. Total protein was determined using a colorimetric method. After protein precipitation, 10 μg/sample was digested using a 1:25 trypsin:sample ratio, according to a method previously described [19]. After digestion, samples were desalted using ZipTip (Merck) according to manufacturer instructions.

Targeted nanoLC-MS/MS analyses were performed on a 1D Plus nanoLC Ultra system (Eksigent, Dublin, CA, USA) interfaced to a Sciex 5500 QTRAP triple quadrupole mass spectrometer (Sciex, Framingham, MA, USA) equipped with a nano-ESI source and controlled by Analyst v.1.5.2. software (ABSciex), according to Mora MI *et al.* [20].

2.4. Western blotting

Pancreatic tissues were frozen at −80 °C until homogenization in extraction buffer (100 mg/ml) on ice. The extraction buffer contained 20 mM Tris–HCl (pH 7.5), 1 mM EDTA, 150 mM NaCl, 0.1% SDS, 1% Igepal CA-630, 30 mM sodium pyrophosphate, 50 mM sodium fluoride, 50 μM sodium orthovanadate (all from Sigma-Aldrich, St. Louis, MO, USA) and a protease inhibitor cocktail (Sigma-Aldrich, St. Louis, MO, USA) at a concentration of 0.4% (v/v). For western blotting under non-reducing conditions, 50 mM NEM was added to the extraction buffer. Protein extracts were added to reducing or non-reducing sample buffer and separated by SDS-PAGE. For electrophoresis under reducing conditions, the following sample buffer was used: 130 mM Tris–HCl, pH 6.8, 10% glycerol, 0.05% bromophenol blue, 2% SDS, and 100 mM DTT. When electrophoresis was performed under non-reducing

conditions, the sample buffer had the same composition but without DTT. The following antibodies were used: anti-CBS (1:1000; Cell Signalling Technology, Danvers, MA, USA), anti-nitro-tyrosine (Cell Signaling Technology, Danvers, MA, USA) and anti-beta tubulin (1:1000, Abcam, Cambridge, UK).

2.5. Immunoprecipitation

Tissue extracts were prepared and subjected to immunoprecipitation with specific antibody against CBS as previously described [21]. The immunoprecipitates were assessed for the presence of nitro-tyrosine by western blotting with anti-nitro-tyrosine antibody.

2.6. RT-qPCR analysis of the gene expression

A piece of around 30 mg of pancreas was excised and immediately immersed in RNA-later solution (Ambion, Thermo Fisher Scientific, Waltham, MA, USA) to stabilize the RNA. The isolated RNA (2 mg/lane) was size-fractionated by electrophoresis in a 1% agarose/formalin gel, and stained with ethidium bromide to assess the quality of the RNA. The cDNA used as template for amplification in the PCR assay was obtained by the reverse transcription reaction using SuperScript II (Invitrogen, Carlsbad, CA, USA), with random hexamers as primers, starting with equal amounts of RNA [22]. The RNA level of the genes was analyzed by dsDNA binding dye Syber Green PCR Master mix in an iQTM5 Multicolor Real-Time PCR Detection System (Biorad Laboratories, Hercules, CA, USA). Each reaction was run in triplicate, and the melting curves were constructed using Dissociation Curves Software (Bio-Rad Laboratories, Hercules, CA, USA) to ensure that only a single product was amplified. The specific primers used are shown in Table 2. The threshold cycle (C_T) was determined and the relative gene expression was expressed as follows: fold change = $2_T^{-\Delta(\Delta C)}$, where $\Delta C_T = C_{T\ target} - C_{T\ housekeeping}$, and $\Delta(\Delta C_T) = \Delta C_{T\ treated} - \Delta C_{T\ control}$. *Tbp* was used as housekeeping gene to normalize the transcription analysis.

2.7. Chromatin immunoprecipitation assay (ChIP)

Chromatin from frozen pancreatic tissues was isolated as described in [22]. Briefly, 37% formaldehyde was used to crosslink 100 mg of pancreas tissue during 10 min. For fragmentation, chromatin was subjected to 7 cycles of 5 min sonication (30 s on, 30 s off) in a Bioruptor Plus instrument (Diagenode, Seraing, Belgium). Under these conditions, the average size of chromatin fragments was 500 ± 200 bp. EZ-Magna ChIP HiSens Chromatin Immunoprecipitation Kit (Millipore, Burlington, MA, USA) was then used to immunoprecipitate the chromatin fragments as described by the manufacturer. The antibody against H3K4me3 (Millipore, Burlington, MA, USA) was used for immunoprecipitation and an aliquot without antibody was used as a negative ChIP assay control. Immunoprecipitated DNA was purified with a PCR purification kit (Qiagen, Hilden, Germany) and analyzed by qPCR using oligonucleotides designed from the promoter regions of *Tnf-α*, *Il-6,* and *Nos2* genes (Table 3).

Table 2
Oligonucleotides used for RT-PCR.

Target gene	TaqMan®probe
Tnf-α	Mm00443258_g1
Il-6	Mm00446190_m1
Tbp	Mm01277042_m1
Target gene	**Forward/reverse oligonucleotide**
Nos1	5′- GTCCTCAGCAAGGGGCTTC-3′
	5′- GGAATAGTAGCGAGGTTGTAGCA-3′
Nos2	5′- GCATCCCAAGTACGAGTGGGT-3′
	5′- GAAGTCTCGAACTCCAATC-3′
Nos3	5′- AGTTACCAGCTGGCCAAAGT-3′
	5′- AGGAGTTAGGCTGCCTGAGA-3′
Tbp	5′- CAGCCTTCCACCTTATGCTC - 3′
	5′- CCGTAAGGCATCATTGGACT -3′

Table 3
Oligonucleotides used for ChIP.

Target gene	Direct/reverse oligonucleotide
Tnf-α	5′- CTCCCAGAGACATGGTGGAT -3′
	5′- CACCCTCCCACTCCTAAACA - 3′
Il-6	5′- GCGTGCCTGCGTTTAAATA -3′
	5′- AGGAAGGGGAAAGTGTGCTT -3′
Nos2	5′- CCAGAACAAAATCCCTCAGC -3′
	5′- CTCATGCAAGGCCATCTCTT -3′

2.8. Histological analysis

Pieces of pancreas were rapidly removed, fixed in 4% paraformaldehyde (Sigma-Aldrich, St. Louis, MO, USA) for 24 h, and embedded in paraffin (Sigma-Aldrich, St. Louis, MO, USA). 4 μm sections were prepared using an automatic microtome and then stained with hematoxylin and eosin (Sigma-Aldrich, St. Louis, MO, USA) for microscopic analysis. Pancreatic sections were assessed at 20× objective magnification over 10 separate fields for severity of pancreatitis by scoring for edema and inflammatory infiltrate according to the procedure of Van Laethem *et al.* [23].

2.9. Statistical analysis

Results are expressed as mean ± standard deviation (SD). Statistical analysis was performed in two steps. One-way analysis of variance (ANOVA) was performed first. When the overall comparison of groups was significant, differences between individual groups were investigated using the Bonferroni test.

3. Results

3.1. AP caused severe depletion of methionine, SAM, MTA, cystathionine, cysteine and GSH in pancreas

In order to assess the status of the methionine cycle in pancreatic tissue during the time course of acute pancreatitis, we measured the levels of methionine metabolites in pancreas of mice in cerulein-induced acute pancreatitis at 1, 3, 5 and 7 h.

Early after the first cerulein injection (1 h), pancreatic levels of methionine were depleted by 50%, and this depletion was aggravated (by 80%) after 3 h of the first cerulein injection maintaining these low levels thereafter (Fig. 1A). Pancreatic SAM levels remained unchanged during the first hour but exhibited a marked decrease (50%) after the third hour (Fig. 1B). Pancreatic MTA levels increased significantly 1 h after the first cerulein injection, but progressively diminished after this time point (Fig. 1C). In contrast, both pancreatic SAH and homocysteine levels remained unchanged during cerulein-induced acute pancreatitis (Fig. 1D, E).

To assess if homocysteine metabolism was impaired through the trans-sulfuration pathway in acute pancreatitis, we measured cystathionine, cysteine, and glutathione levels in pancreas during cerulein-induced acute pancreatitis by mass spectrometry. Both cystathionine and cysteine levels markedly diminished 1 h after pancreatitis induction, and glutathione levels began to be also markedly depleted after 3 h (Fig. 1F, G, H).

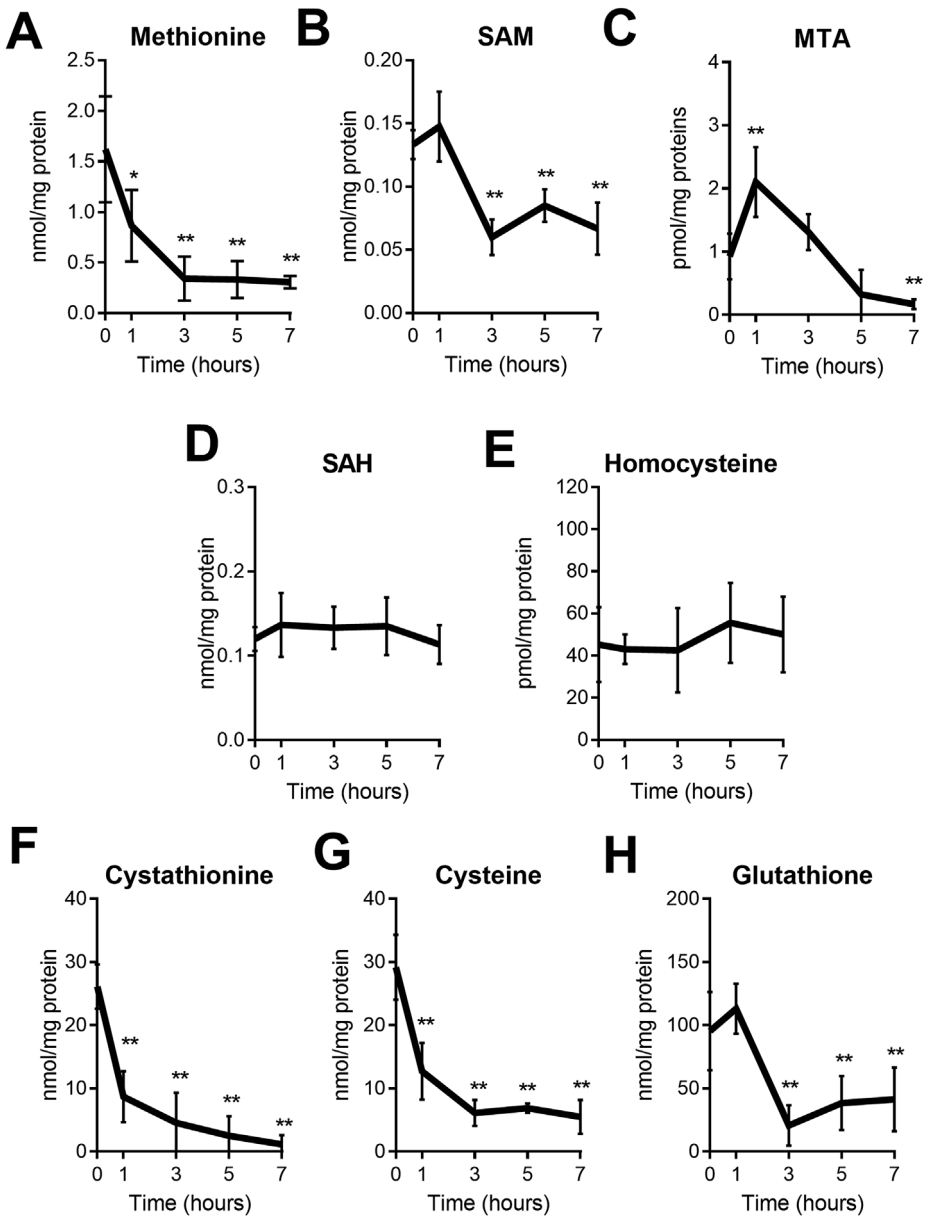

Fig. 1. Levels of methionine (A), S-adenosylmethionine (SAM) (B), methylthioadenosine (MTA) (C), S-adenosylhomocysteine (SAH) (D), homocysteine (E), cystathionine (F), cysteine (G) and reduced glutathione (GSH) (H) in pancreas of control mice and 1 h after the first, third, fifth and seventh injections of cerulein. The number of mice per group was 4–6. Statistical significance is indicated as *p < 0,05 and **p < 0,01.

3.2. AP diminished SAHH and CGL protein levels but increased MTAP protein levels in pancreas

In pancreatic tissue, we analyzed by proteomics the steady-state protein levels of 10 enzymes involved in methionine cycle and transsulfuration pathway (Fig. 2A). Protein levels of methionine adenosyltransferase 1A (MAT1A), MAT2A and MAT2B, the enzymes that regulate the synthesis of SAM from methionine, as well as glycine N-methyltransferase (GNMT), remained unchanged in pancreas with acute pancreatitis (Fig. 2B, C). Pancreatic levels of S-adenosylhomocysteine-hydrolase (SAHH) and cystathionine gamma-lyase (CGL), the enzymes that catalyze the conversion of SAH into homocysteine and cystathionine into cysteine, respectively, were reduced upon cerulein-induced acute pancreatitis (Fig. 2D, F). However, protein levels of cystathionine-β-synthase (CBS) and methionine synthase (MS), the enzymes that catalyze the condensation of homocysteine and serine to form cystathionine, and the re-methylation of homocysteine to methionine, respectively, remained unchanged in pancreas with acute pancreatitis (Fig. 2E, G). In contrast, the pancreatic expression of methylthioadenosine phosphorylase (MTAP), a critical enzyme for the methionine salvage pathway, was increased in mice with cerulein-induced acute pancreatitis (Fig. 2H).

3.3. AP induced gene expression and protein levels of NOS2 and triggered tyrosine nitration of CBS in pancreas

It has been reported that thiol oxidation as well as tyrosine nitration of CBS may compromise its enzymatic activity [24,25]. Thiol oxidation of CBS was not found in pancreas with acute pancreatitis (Fig. S1A), whereas CBS nitration was remarkably increased and accordingly *Nos2* gene expression and its protein levels were markedly up-regulated in pancreas upon cerulein-induced acute pancreatitis (Fig. 3A,B,C). However, mRNA levels of *Nos1* and *Nos3* did not change significantly in acute pancreatitis (Fig. 3A). Supplementary Fig. S2 shows the general

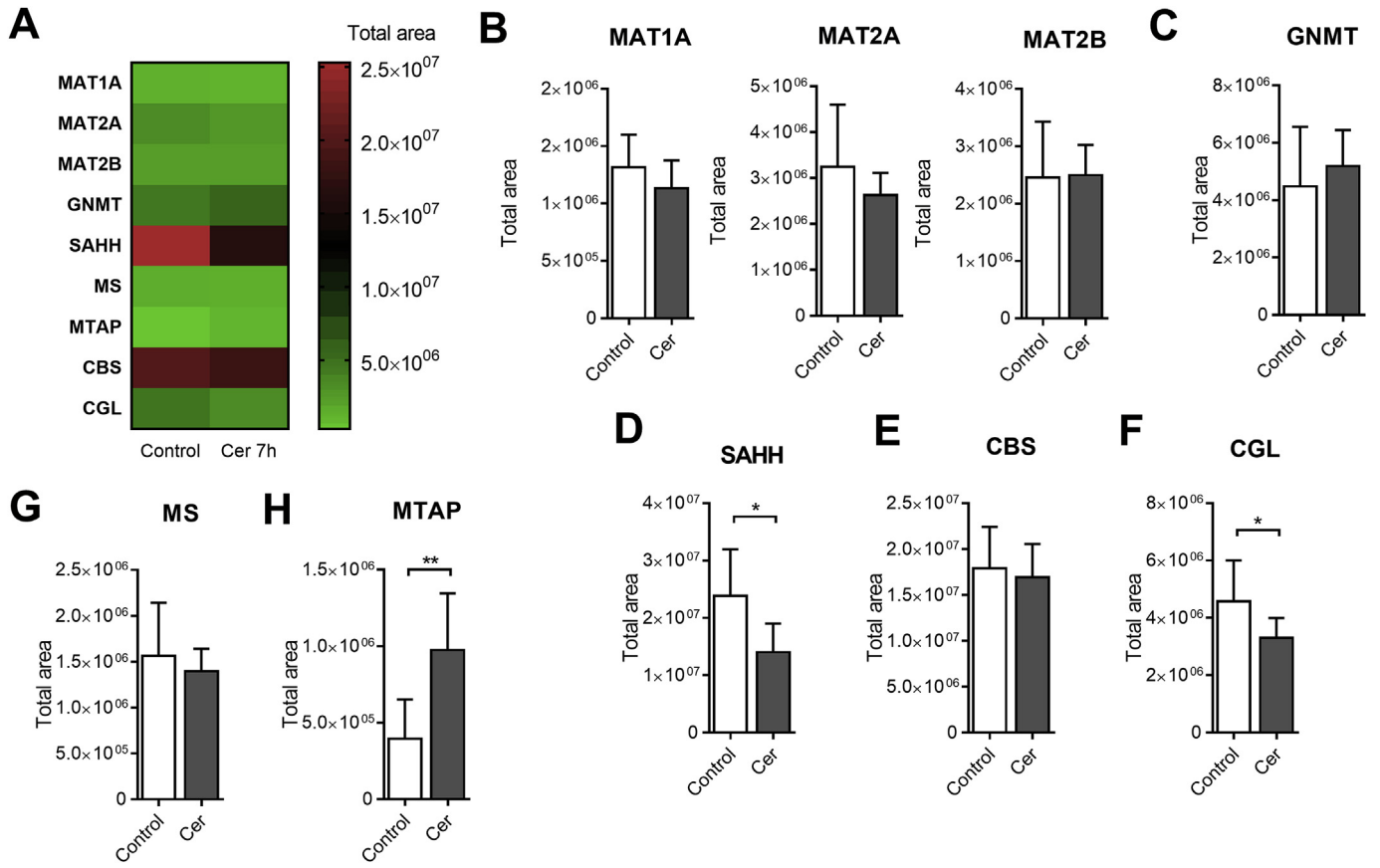

Fig. 2. Heatmap showing the levels of MAT1A, MAT2A, MAT2B, GNMT, SAHH, MS, MTAP, CBS, CGL in pancreas of control mice (Control) and in mice with acute pancreatitis (1 h after seventh injections of cerulein) (Cer) (A). Histograms showing the levels of MAT1A, MAT2A and MAT2B (B), GNMT (C), SAHH (D), CBS (E), CGL (F), MS (G), and MTAP (H), in pancreas of control mice (Control) and in mice with acute pancreatitis (1 h after seventh injections of cerulein) (Cer). The number of mice per group was 6–8. Statistical significance is indicated as *p < 0,05 and **p < 0,01.

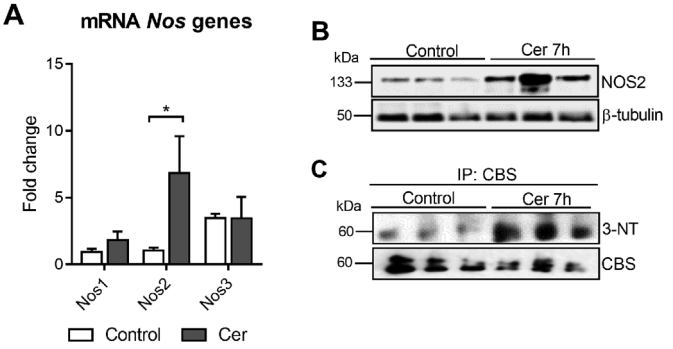

Fig. 3. mRNA relative expression of *Nos1, Nos2* and *Nos3* vs *Tbp* in pancreas of control mice (Control) and in acute pancreatitis (1 h after seventh injections of cerulein) (Cer) (A). Western blot of NOS2 in pancreas of control mice (Control) and in acute pancreatitis (1 h after seventh injections of cerulein) (Cer) (B). Western blot of 3-nitrotyrosine in CBS immunoprecipitate of pancreas of control mice (Control) and in acute pancreatitis (1 h after seventh injections of cerulein) (Cer) (C). The number of mice per group was 4–6. Statistical significance is indicated as *p < 0,05 and **p < 0,01.

level of protein nitration in pancreatic tissue in mice with cerulein-induced acute pancreatitis.

Additionally, serine deficiency may also act as a limiting factor for CBS enzyme activity. However, pancreatic serine levels remained unchanged upon cerulein-induced acute pancreatitis (Fig. S1B).

3.4. SAM administration triggered homocysteine accumulation and aggravated the inflammatory response in AP

In order to confirm the blockade of homocysteine metabolism during cerulein-induced acute pancreatitis, SAM was administered. Thus, pancreatic levels of methionine metabolites 1 h after the last cerulein injection were determined.

Under basal conditions, the group of control mice that received SAM injections (SAM-treated mice) exhibited high levels of SAM and MTA in pancreas in comparison with control mice at time 0. However, pancreatic levels of SAM and MTA diminished not only in mice with pancreatitis (Cer mice) but also in SAM-treated mice with pancreatitis (Cer + SAM mice) (Fig. 4A, B). Additionally, SAH levels were low in pancreas of SAM-treated mice with pancreatitis (Cer + SAM mice) compared with control mice at time 0 and mice with pancreatitis (Fig. 4C).

In contrast with other methionine metabolites, pancreatic homocysteine levels were markedly increased in SAM-treated mice with pancreatitis (Cer + SAM mice) in comparison with all the other experimental groups (Fig. 4D). The impairment of homocysteine re-methylation to methionine during acute pancreatitis was corroborated by measuring methionine levels in pancreatic tissue. Indeed, both mice with pancreatitis (Cer mice) and SAM-treated mice with pancreatitis (Cer + SAM mice) exhibited diminished methionine levels in pancreas in comparison with control mice (Fig. 4E). In addition, treatment with SAM did not modify the pancreatic levels of cystathionine, cysteine, and GSH in SAM-treated mice with pancreatitis compared with those mice without treatment. Thus, the levels of these metabolites remained low in these two experimental groups with pancreatitis compared with

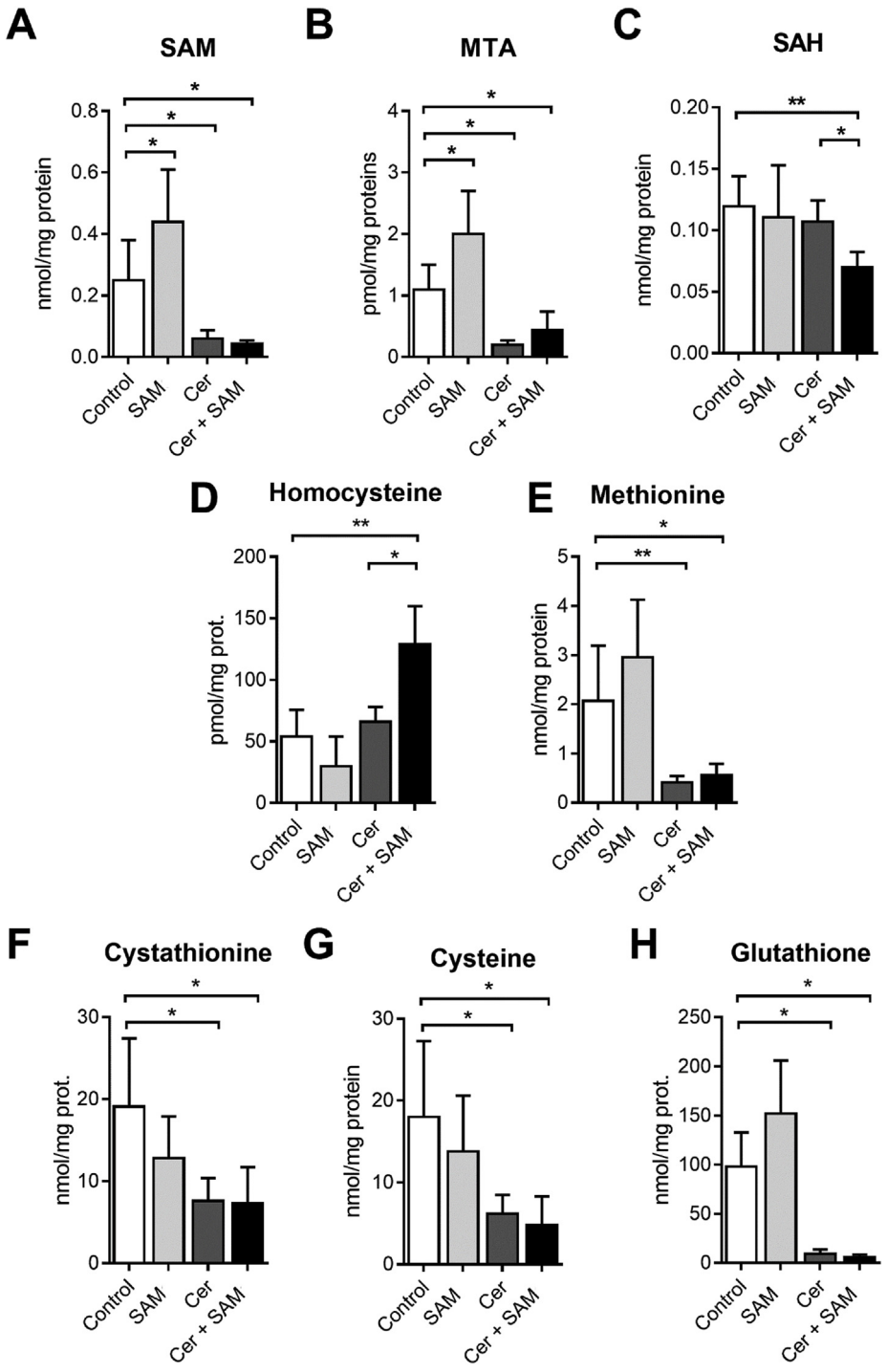

Fig. 4. Levels of S-adenosylmethionine (SAM) (A), methylthioadenosine (MTA) (B), S-adenosylhomocysteine (SAH) (C), homocysteine (D), methionine (E), cystathionine (F), cysteine (G) and reduced glutathione (GSH) (H) in pancreas of control mice (Control), SAM-treated control mice (SAM), mice with acute pancreatitis (1 h after seventh injections of cerulein) (Cer) and SAM-treated mice with acute pancreatitis (1 h after seventh injections of cerulein) (Cer + SAM). The number of mice per group was 4–6. Statistical significance is indicated as *p < 0,05 and **p < 0,01.

control mice (Fig. 4F, G, H).

To evaluate the impact of SAM treatment on the inflammatory response during acute pancreatitis, *Tnf-α* and *Il-6* gene expression were measured. As expected, *Tnf-α* and *Il*-6 mRNA levels were dramatically increased in acute pancreatitis, but their gene expression was even higher in SAM-treated mice with pancreatitis in comparison with untreated mice with pancreatitis (Fig. 5A). Furthermore, we performed CHIP assay to determine the presence of the euchromatin marker H3K4me3 at the promoter region of *Tnf-α* and *Il-6* genes. We found that the promoter regions of these two genes were enriched in H3K4me3 in SAM-treated mice with pancreatitis in comparison with SAM-untreated mice with pancreatitis (Fig. 5B).

Histological analysis of the pancreatic tissue revealed that both inflammatory infiltrate and edema were more intense in SAM-treated mice with pancreatitis in comparison with SAM-untreated mice with pancreatitis (Fig. 5C).

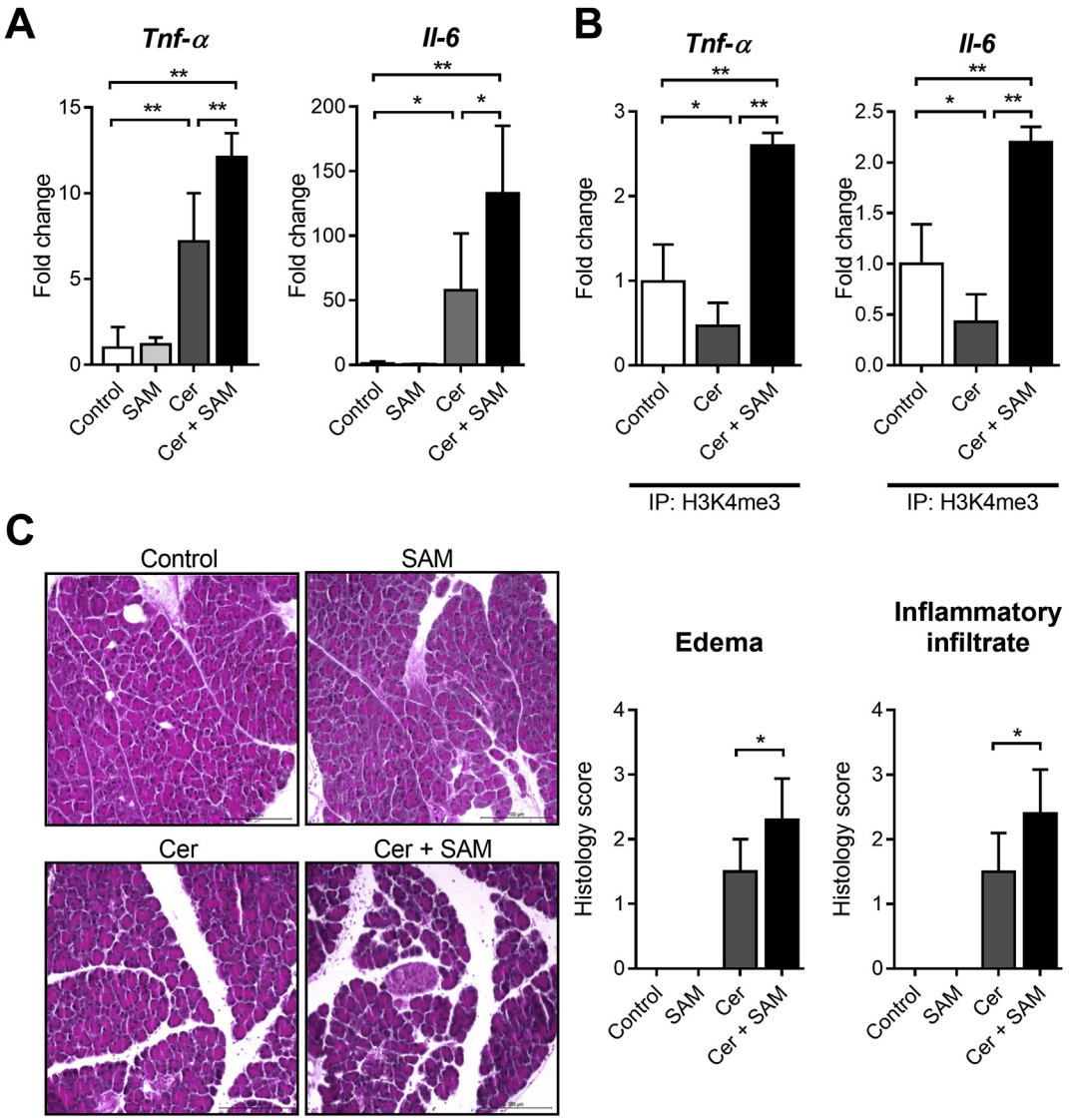

Fig. 5. mRNA relative expression of *Tnf-α* and *Il6* vs *Tbp* in pancreas of control mice (Control), SAM-treated control mice (SAM), mice with acute pancreatitis (1 h after seventh injections of cerulein) (Cer) and SAM-treated mice with acute pancreatitis (1 h after seventh injections of cerulein) (Cer + SAM) (A). H3K4me3 levels in the promoter of *Tnf-α* and *Il6* in pancreas of control mice (Control), in mice with acute pancreatitis (1 h after seventh injections of cerulein) (Cer) and in SAM-treated mice with acute pancreatitis (1 h after seventh injections of cerulein) (Cer + SAM) measured by ChIP assay (B). Representative histology and histological scores for edema and inflammatory infiltrate in pancreas of control mice (Control), SAM-treated control mice (SAM), mice with acute pancreatitis (1 h after seventh injections of cerulein) (Cer) and SAM-treated mice with acute pancreatitis (1 h after seventh injections of cerulein) (Cer + SAM) (C). The number of mice per group was 4–6. Statistical significance is indicated as * p < 0,05 and **p < 0,01.

3.5. SAM administration enhanced Nos2 gene expression and CBS nitration in pancreas in AP

Nos2 gene expression was higher in SAM-treated mice with pancreatitis in comparison with untreated mice with pancreatitis (Fig. 6A). Similarly to *Tnf-α* and *Il-6,* H3K4me3 was increased too in the promoter region of *Nos2* in SAM-treated mice with pancreatitis in comparison with untreated mice with pancreatitis (Fig. 6B). To assess the impact of *Nos2* up-regulation on CBS nitration, we measured tyrosine nitration of CBS in SAM-treated mice with pancreatitis (Cer + SAM). Indeed, SAM treatment increased nitrated levels of CBS in pancreas of mice with acute pancreatitis (Fig. 6C).

4. Discussion

In the present work, we show that nitrosative stress dysregulates methionine metabolism in pancreas in acute pancreatitis directly affecting the trans-sulfuration pathway. Our results show a progressive depletion in pancreatic levels of methionine with parallel decrease in cystathionine and cysteine. SAM and glutathione levels were also rapidly depleted in pancreas during experimental acute pancreatitis in accordance with previous reports [16,17]. In this work, we have also found that pancreatic SAH and homocysteine levels remain unchanged upon cerulein-induced acute pancreatitis. We have identified the cause of this dysregulation showing that tyrosine-nitration of CBS seems to be responsible for blockade of the trans-sulfuration in experimental acute pancreatitis. Therefore, in acute pancreatitis CBS nitration impairs homocysteine metabolism and limits metabolic flux through this pathway.

CBS is a tetrameric redox-sensitive and rate-limiting enzyme responsible for homocysteine conversion to cystathionine. CBS activity is allosterically activated by SAM [26] and S-glutathionylation [27] but inhibited by CO [28,29] and NO [30,31]. Thus, the redox status of the heme cofactor has been reported as a central redox modulator of CBS

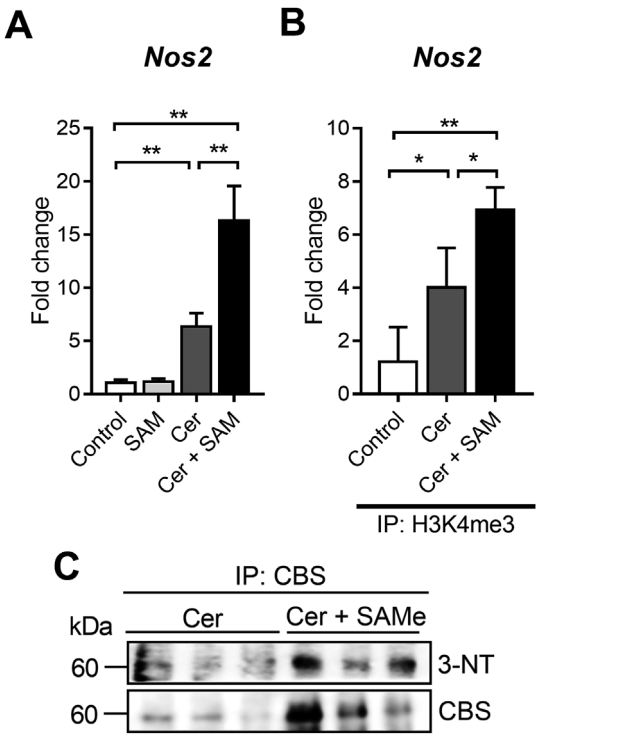

Fig. 6. mRNA relative expression of *Nos2* vs *Tbp* in pancreas of control mice (Control), SAM-treated control mice (SAM), mice with acute pancreatitis (1 h after seventh injections of cerulein) (Cer) and SAM-treated mice with acute pancreatitis (1 h after seventh injections of cerulein) (Cer + SAM) (A). H3K4me3 levels in the promoter of *Nos2* in pancreas of control mice (Control), in mice with acute pancreatitis (1 h after seventh injections of cerulein) (Cer), and in SAM-treated mice with acute pancreatitis (1 h after seventh injections of cerulein) (Cer + SAM) measured by ChIP assay (B). Western blot of 3-nitrotyrosine in CBS immunoprecipitate of pancreas of mice with acute pancreatitis (1 h after seventh injections of cerulein) (Cer) and SAM-treated mice with acute pancreatitis (1 h after seventh injections of cerulein) (Cer + SAM) (C). The number of mice per group was 4–6. Statistical significance is indicated as *p < 0,05 and **p < 0,01.

activity. The ferrous form of CBS exhibits lower activity than the ferric form of CBS [32]. Nevertheless, due to the low heme redox potential (−350 mV), the existence of ferrous CBS state is controversial under physiological conditions [25,33]. Recently, it has been reported that a redox-active disulfide bond modulates CBS activity [25]. However, we have not found thiol oxidation of CBS in acute pancreatitis. It is noteworthy that the levels of tyrosine-nitrated CBS were markedly increased in this model of acute inflammation. Nitration-mediated loss of CBS activity associated with elevated levels of homocysteine has been previously reported in aging rats [24]. In addition, *in vitro* experiments have shown that peroxynitrite ($ONOO^-$) may inactivate CBS activity [34]. Accordingly, pre-treatment with $ONOO^-$ scavenger FeTMPyP prevented CBS nitration and ameliorated homocysteine accumulation in aging rats [24]. In our model, CBS nitration impairs homocysteine metabolism through the trans-sulfuration pathway restraining GSH biosynthesis. It is known that up-regulation of *Nos2* expression triggers nitrosative stress in pancreas with acute pancreatitis [35,36] as it occurs generally in acute inflammation. Hence, pancreatic levels of nitrotyrosine, a marker of nitrosative stress, increased in mice with cerulein-induced acute pancreatitis [37–39]. Our results confirm the increased *Nos2* expression and show the detrimental effect of nitrosative stress on the trans-sulfuration pathway in acute pancreatitis, and specifically on CBS regulation. Furthermore, in accordance with other studies our results suggest that *Nos2*, but not *Nos1* or *Nos3*, is the main source of NO and the major contributor to nitrosative stress during acute pancreatitis [36,37]. In fact, *Nos2*-deficient mice exhibited a reduced degree of pancreatic inflammation and tissue injury in pancreas with acute pancreatitis [37]. In contrast and strikingly, genetic deletion of *Nos3* aggravated the severity of acute pancreatitis in mice [40]. Hence, here we are proposing that *Nos2* up-regulation triggers CBS nitration and blockade in the metabolism of homocysteine in pancreas during acute pancreatitis.

CBS nitration might be widely associated with inflammation as this would explain the increased levels of homocysteine found in a variety of inflammatory disorders, including inflammatory bowel disease [7,8], and vascular inflammation [41]. Furthermore, the elevated levels of homocysteine would contribute to severity of inflammatory diseases promoting oxidative stress, endothelial dysfunction, and cardiovascular disease [41–43].

CBS is also involved in the synthesis of hydrogen sulfide (H_2S) together with cystathionine gamma-lyase (CGL) and mercaptopyruvate sulfurtransferase [44]. CGL is the major enzyme responsible for H_2S synthesis in pancreas during pancreatitis [44] so the contribution of CBS in this regard is likely to be minor. The role of H_2S in inflammation is still controversial as it may exert opposite effects on the inflammatory response depending on the tissue, its concentration and its source [45–48]. Endogenous H_2S seems to exert a pro-inflammatory role in pancreatitis as GCL knock-out mice exhibited less pancreatic edema, inflammatory infiltrate, and acinar necrosis in acute pancreatitis [44].

CBS nitration may directly limit the ability of exogenous SAM to modulate the trans-sulfuration pathway and GSH levels in experimental acute pancreatitis. Unexpectedly, we have found that SAM administration increased *Nos2* expression and CBS nitration in this inflammatory process. Consequently, homocysteine is accumulated in pancreas during acute pancreatitis upon SAM treatment.

Although it is known that SAM supplementation exhibits hepatoprotective effects against liver injury and may provide beneficial effects ameliorating inflammation-induced colon cancer in mice [4,49], we show here that SAM treatment clearly exhibits a pro-inflammatory effect in acute pancreatitis in mice suggesting that SAM administration in acute inflammatory disorders may not be beneficial. Our results demonstrate that SAM supplementation increased the euchromatin marker tri-methylated K4 of histone 3 (H3K4me3), a signature for active transcription, in the promoter regions of *Tnf-α*, *Il-6* and *Nos2* genes and enhanced their up-regulation in mice with acute pancreatitis. These findings suggest that SAM supplementation may increase histone methylation in the promoters of pro-inflammatory genes inducing their expression. Consequently, acute pancreatitis was aggravated upon SAM administration and indeed, we found more intense edema and inflammatory infiltrate in the pancreas of SAM-treated mice with pancreatitis.

In conclusion, acute pancreatitis causes blockade of the trans-sulfuration pathway mediated by nitration of cystathionine β-synthase, which is enhanced by administration of S-adenosylmethionine. Our results highlight for the first time the adverse effects of nitrosative stress in acute inflammation through CBS nitration and impairment of homocysteine metabolism. Hence, in this work we provide new insights to understand the mechanisms, not yet fully elucidated, that lead to increased levels of homocysteine in inflammatory disorders.

Conflicts of interest

The authors declare that there are no conflict of interest.

Acknowledgements and Funding Source

This work was supported by Grant SAF2015-71208-R with FEDER funds from the Spanish Ministry of Economy and Competitiveness to J.S.

Appendix A. Supplementary data

Supplementary data to this article can be found online at https://doi.org/10.1016/j.redox.2019.101324.

References

[1] M.V. Martinov, V.M. Vitvitsky, R. Banerjee, F.I. Ataullakhanov, The logic of the hepatic methionine metabolic cycle, Biochim. Biophys. Acta 1804 (2010) 89–96.

[2] C.D. Tavares, K. Sharabi, J.E. Dominy, Y. Lee, M. Isasa, J.M. Orozco, M.P. Jedrychowski, T.M. Kamenecka, P.R. Griffin, S.P. Gygi, P. Puigserver, The methionine transamination pathway controls hepatic glucose metabolism through regulation of the GCN5 acetyltransferase and the PGC-1alpha transcriptional coactivator, J. Biol. Chem. 291 (2016) 10635–10645.

[3] D. Thomas, A. Becker, Y. Surdin-Kerjan, Reverse methionine biosynthesis from S-adenosylmethionine in eukaryotic cells, J. Biol. Chem. 275 (2000) 40718–40724.

[4] S.C. Lu, J.M. Mato, S-adenosylmethionine in liver health, injury, and cancer, Physiol. Rev. 92 (2012) 1515–1542.

[5] K. Soda, Polyamine metabolism and gene methylation in conjunction with one-carbon metabolism, Int. J. Mol. Sci. 19 (2018) 3106, https://doi.org/10.3390/ijms19103106. eCollection 2018 Oct.

[6] M.A. Pajares, D. Perez-Sala, Mammalian sulfur amino acid metabolism: a nexus between redox regulation, nutrition, epigenetics, and detoxification, Antioxidants Redox Signal. 29 (2018) 408–452.

[7] S. Danese, A. Sgambato, A. Papa, F. Scaldaferri, R. Pola, M. Sans, M. Lovecchio, G. Gasbarrini, A. Cittadini, A. Gasbarrini, Homocysteine triggers mucosal microvascular activation in inflammatory bowel disease, Am. J. Gastroenterol. 100 (2005) 886–895.

[8] Y. Chowers, B.A. Sela, R. Holland, H. Fidder, F.B. Simoni, S. Bar-Meir, Increased levels of homocysteine in patients with crohn's disease are related to folate levels, Am. J. Gastroenterol. 95 (2000) 3498–3502.

[9] S.P.K. Shiao, A. Lie, C.H. Yu, Meta-analysis of homocysteine-related factors on the risk of colorectal cancer, Oncotarget 9 (2018) 25681–25697.

[10] S.H. Rahman, A.R. Srinivasan, A. Nicolaou, Transsulfuration pathway defects and increased glutathione degradation in severe acute pancreatitis, Dig. Dis. Sci. 54 (2009) 675–682.

[11] S. Perez, J. Pereda, L. Sabater, J. Sastre, Redox signaling in acute pancreatitis, Redox Biol. 5 (2015) 1–14.

[12] B.A. Neuschwander-Tetri, L.D. Ferrell, R.J. Sukhabote, J.H. Grendell, Glutathione monoethyl ester ameliorates caerulein-induced pancreatitis in the mouse, J. Clin. Investig. 89 (1992) 109–116.

[13] J. Pereda, J. Escobar, J. Sandoval, J.L. Rodriguez, L. Sabater, F.V. Pallardo, L. Torres, L. Franco, J. Vina, G. Lopez-Rodas, J. Sastre, Glutamate cysteine ligase up-regulation fails in necrotizing pancreatitis, Free Radic. Biol. Med. 44 (2008) 1599–1609.

[14] S.H. Rahman, K. Ibrahim, M. Larvin, A. Kingsnorth, M.J. McMahon, Association of antioxidant enzyme gene polymorphisms and glutathione status with severe acute pancreatitis, Gastroenterology 126 (2004) 1312–1322.

[15] M.L. Moreno, J. Escobar, A. Izquierdo-Alvarez, A. Gil, S. Perez, J. Pereda, I. Zapico, M. Vento, L. Sabater, A. Marina, A. Martinez-Ruiz, J. Sastre, Disulfide stress: a novel type of oxidative stress in acute pancreatitis, Free Radic. Biol. Med. 70 (2014) 265–277.

[16] S.C. Lu, I. Gukovsky, A. Lugea, C.N. Reyes, Z.Z. Huang, L. Chen, J.M. Mato, T. Bottiglieri, S.J. Pandol, Role of S-adenosylmethionine in two experimental models of pancreatitis, FASEB J. 17 (2003) 56–58.

[17] S. Perez, S. Rius-Perez, I. Finamor, P. Marti-Andres, I. Prieto, R. Garcia, M. Monsalve, J. Sastre, Obesity causes PGC-1alpha deficiency in the pancreas leading to marked IL-6 upregulation via NF-kappaB in acute pancreatitis, J. Pathol. 247 (2019) 48–59.

[18] J. Escobar, A. Sanchez-Illana, J. Kuligowski, I. Torres-Cuevas, R. Solberg, H.T. Garberg, M.U. Huun, O.D. Saugstad, M. Vento, C. Chafer-Pericas, Development of a reliable method based on ultra-performance liquid chromatography coupled to tandem mass spectrometry to measure thiol-associated oxidative stress in whole blood samples, J. Pharm. Biomed. Anal. 123 (2016) 104–112.

[19] D. Lopez-Ferrer, S. Martinez-Bartolome, M. Villar, M. Campillos, F. Martin-Maroto, J. Vazquez, Statistical model for large-scale peptide identification in databases from tandem mass spectra using SEQUEST, Anal. Chem. 76 (2004) 6853–6860.

[20] M.I. Mora, M. Molina, L. Odriozola, F. Elortza, J.M. Mato, B. Sitek, P. Zhang, F. He, M.U. Latasa, M.A. Avila, F.J. Corrales, Prioritizing popular proteins in liver cancer: remodelling one-carbon metabolism, J. Proteome Res. 16 (2017) 4506–4514.

[21] M. Monsalve, Z. Wu, G. Adelmant, P. Puigserver, M. Fan, B.M. Spiegelman, Direct coupling of transcription and mRNA processing through the thermogenic coactivator PGC-1, Mol. Cell 6 (2000) 307–316.

[22] J. Sandoval, J. Pereda, S. Perez, I. Finamor, A. Vallet-Sanchez, J.L. Rodriguez, L. Franco, J. Sastre, G. Lopez-Rodas, Epigenetic regulation of early- and late-response genes in acute pancreatitis, J. Immunol. 197 (2016) 4137–4150.

[23] J.L. Van Laethem, R. Eskinazi, H. Louis, F. Rickaert, P. Robberecht, J. Deviere, Multisystemic production of interleukin 10 limits the severity of acute pancreatitis in mice, Gut 43 (1998) 408–413.

[24] H. Wang, Q. Sun, Y. Zhou, H. Zhang, C. Luo, J. Xu, Y. Dong, Y. Wu, H. Liu, W. Wang, Nitration-mediated deficiency of cystathionine beta-synthase activity accelerates the progression of hyperhomocysteinemia, Free Radic. Biol. Med. 113 (2017) 519–529.

[25] W. Niu, J. Wang, J. Qian, M. Wang, P. Wu, F. Chen, S. Yan, Allosteric control of human cystathionine beta-synthase activity by a redox active disulfide bond, J. Biol. Chem. 293 (2018) 2523–2533.

[26] J. Ereno-Orbea, T. Majtan, I. Oyenarte, J.P. Kraus, L.A. Martinez-Cruz, Structural insight into the molecular mechanism of allosteric activation of human cystathionine beta-synthase by S-adenosylmethionine, Proc. Natl. Acad. Sci. U. S. A 111 (2014) E3845–E3852.

[27] W.N. Niu, P.K. Yadav, J. Adamec, R. Banerjee, S-glutathionylation enhances human cystathionine beta-synthase activity under oxidative stress conditions, Antioxidants Redox Signal. 22 (2015) 350–361.

[28] S. Taoka, M. West, R. Banerjee, Characterization of the heme and pyridoxal phosphate cofactors of human cystathionine beta-synthase reveals nonequivalent active sites, Biochemistry 38 (1999) 2738–2744.

[29] M. Puranik, C.L. Weeks, D. Lahaye, O. Kabil, S. Taoka, S.B. Nielsen, J.T. Groves, R. Banerjee, T.G. Spiro, Dynamics of carbon monoxide binding to cystathionine beta-synthase, J. Biol. Chem. 281 (2006) 13433–13438.

[30] S. Taoka, R. Banerjee, Characterization of NO binding to human cystathionine beta-synthase: possible implications of the effects of CO and NO binding to the human enzyme, J. Inorg. Biochem. 87 (2001) 245–251.

[31] J.B. Vicente, H.G. Colaco, M.I. Mendes, P. Sarti, P. Leandro, A. Giuffre, NO* binds human cystathionine beta-synthase quickly and tightly, J. Biol. Chem. 289 (2014) 8579–8587.

[32] S. Taoka, S. Ohja, X. Shan, W.D. Kruger, R. Banerjee, Evidence for heme-mediated redox regulation of human cystathionine beta-synthase activity, J. Biol. Chem. 273 (1998) 25179–25184.

[33] S. Singh, P. Madzelan, J. Stasser, C.L. Weeks, D. Becker, T.G. Spiro, J. Penner-Hahn, R. Banerjee, Modulation of the heme electronic structure and cystathionine beta-synthase activity by second coordination sphere ligands: the role of heme ligand switching in redox regulation, J. Inorg. Biochem. 103 (2009) 689–697.

[34] L. Celano, M. Gil, S. Carballal, R. Duran, A. Denicola, R. Banerjee, B. Alvarez, Inactivation of cystathionine beta-synthase with peroxynitrite, Arch. Biochem. Biophys. 491 (2009) 96–105.

[35] N. Ueno, S. Kashiwamura, H. Ueda, H. Okamura, N.M. Tsuji, K. Hosohara, J. Kotani, S. Marukawa, Role of interleukin 18 in nitric oxide production and pancreatic damage during acute pancreatitis, Shock 24 (2005) 564–570.

[36] A.D. Ang, S. Adhikari, S.W. Ng, M. Bhatia, Expression of nitric oxide synthase isoforms and nitric oxide production in acute pancreatitis and associated lung injury, Pancreatology 9 (2009) 150–159.

[37] S. Cuzzocrea, E. Mazzon, L. Dugo, I. Serraino, T. Centorrino, A. Ciccolo, F.A. Van de Loo, D. Britti, A.P. Caputi, C. Thiemermann, Inducible nitric oxide synthase-deficient mice exhibit resistance to the acute pancreatitis induced by cerulein, Shock 17 (2002) 416–422.

[38] S. Cuzzocrea, B. Pisano, L. Dugo, A. Ianaro, D. Britti, N.S. Patel, R. Di Paola, T. Genovese, M. Di Rosa, A.P. Caputi, C. Thiemermann, Rosiglitazone, a ligand of the peroxisome proliferator-activated receptor-gamma, reduces acute pancreatitis induced by cerulein, Intensive Care Med. 30 (2004) 951–956.

[39] S. Balachandra, T. Genovese, E. Mazzon, R. Di Paola, C. Thiemerman, A.K. Siriwardena, S. Cuzzocrea, Inhibition of tyrosine-kinase-mediated cellular signaling by tyrphostins AG 126 and AG556 modulates murine experimental acute pancreatitis, Surgery 138 (2005) 913–923.

[40] M.J. DiMagno, J.A. Williams, Y. Hao, S.A. Ernst, C. Owyang, Endothelial nitric oxide synthase is protective in the initiation of caerulein-induced acute pancreatitis in mice, Am. J. Physiol. Gastrointest. Liver Physiol. 287 (2004) G80–G87.

[41] L. Papatheodorou, N. Weiss, Vascular oxidant stress and inflammation in hyperhomocysteinemia, Antioxidants Redox Signal. 9 (2007) 1941–1958.

[42] B.A. Maron, J. Loscalzo, The treatment of hyperhomocysteinemia, Annu. Rev. Med. 60 (2009) 39–54.

[43] R.T. Eberhardt, M.A. Forgione, A. Cap, J.A. Leopold, M.A. Rudd, M. Trolliet, S. Heydrick, R. Stark, E.S. Klings, N.I. Moldovan, M. Yaghoubi, P.J. Goldschmidt-Clermont, H.W. Farber, R. Cohen, J. Loscalzo, Endothelial dysfunction in a murine model of mild hyperhomocyst(e)inemia, J. Clin. Investig. 106 (2000) 483–491.

[44] A.D. Ang, S. Adhikari, S.W. Ng, M. Bhatia, Expression of nitric oxide synthase isoforms and nitric oxide production in acute pancreatitis and associated lung injury, Pancreatology 9 (2009) 150–159.

[45] M. Bhatia, F.L. Wong, D. Fu, H.Y. Lau, S.M. Moochhala, P.K. Moore, Role of hydrogen sulfide in acute pancreatitis and associated lung injury, FASEB J. 19 (2005) 623–625.

[46] D. Dal-Secco, T.M. Cunha, A. Freitas, J.C. Alves-Filho, F.O. Souto, S.Y. Fukada, R. Grespan, N.M. Alencar, A.F. Neto, M.A. Rossi, S.H. Ferreira, J.S. Hothersall, F.Q. Cunha, Hydrogen sulfide augments neutrophil migration through enhancement of adhesion molecule expression and prevention of CXCR2 internalization: role of ATP-sensitive potassium channels, J. Immunol. 181 (2008) 4287–4298.

[47] L. Li, M. Salto-Tellez, C.H. Tan, M. Whiteman, P.K. Moore, GYY4137, a novel hydrogen sulfide-releasing molecule, protects against endotoxic shock in the rat, Free Radic. Biol. Med. 47 (2009) 103–113.

[48] J.L. Wallace, L. Vong, W. McKnight, M. Dicay, G.R. Martin, Endogenous and exogenous hydrogen sulfide promotes resolution of colitis in rats, Gastroenterology 137 (2009) 569-78, 578.e1.

[49] T.W. Li, H. Yang, H. Peng, M. Xia, J.M. Mato, S.C. Lu, Effects of S-adenosylmethionine and methylthioadenosine on inflammation-induced colon cancer in mice, Carcinogenesis 33 (2012) 427–435.